Middle East Journal of Applied Science & Technology (MEJAST)
Volume 7, Issue 1, Pages 174-184, January-March 2024

Petrophysical Evaluation of Selected Wells in FUBA Field Reservoir in Niger Delta, Nigeria

U. Ochoma[1*]

[1]*Department of Physics, Rivers State University, P.M.B 5080, Port Harcourt, Nigeria.*
*Corresponding Author Email: umaocho@gmail.com**

DOI: https://doi.org/10.46431/MEJAST.2024.7110

Article Received: 21 December 2023 *Article Accepted: 26 February 2024* *Article Published: 29 March 2024*

ABSTRACT

Petrophysical evaluation of selected wells in FUBA field reservoir in Niger Delta, Nigeria are here presented. A suite of well logs comprising gamma ray, deep resistivity, density, sonic and neutron were used in the analysis. Petrophysical properties evaluated are; thickness, porosity, permeability, water saturation and hydrocarbon saturation. Two distinct horizons were mapped. The lithostratigraphy correlation section revealed that each of the sand units spread over the field differ in thickness with some units occurring at greater depth than their adjacent unit, that is possibly an evidence of faulting. From the result of Petrophysical evaluation, on average, net thickness, effective porosity, permeability, water saturation, hydrocarbon saturation and shale volume values are 13.50 ft, 23.50%, 463.70 mD, 30.50%, 69.50% and 12.50% for reservoir sand Q and 45.00 ft, 22.20%, 495.24 mD, 32% and 68% and 16.50% for reservoir sand R. The porosity and permeability values have been classed as good to excellent for reservoir sand Q and R respectively. The hydrocarbon saturation and water saturation values are good for reservoir development for production. The results of the sand-shale lithology calculated indicate the following (i) the fraction of shale in the reservoirs is quite low; (ii) sandstone volume decreased with increasing depth while shale volume increased with depth; (iii) an inverse relationship between permeability and shale volume and a direct relationship between permeability and the volume of sand in the reservoirs. This is typical of clastic reservoir systems in the Niger Delta. An analysis of the petrophysical attributes maps indicates how the petrophysical qualities vary across the reservoirs. The results for this work revealed the presence of hydrocarbon in both reservoirs across the wells in the study area.

Keywords: Petrophysical evaluation; Petrophysical attributes map; Faults; Niger Delta; Nigeria.

1.0. Introduction

A reservoir is one which by virtue of its porosity and permeability is capable of containing a reasonable quantity of hydrocarbon if entrapment conditions are right, but can also release hydrocarbon at a satisfactory rate when the reservoir is penetrated by a well (Etu-Efeotor, 1997). Integrating log-derived reservoir properties with seismic data and structural interpretation enable an interpretation team to quantify subsurface hydrocarbon accumulations, generate prospects and leads, classify petroleum resources, determine probability of success, rank resources, plan future wells, reduce exploration and drilling risks (Adeoye and Enikanselu 2009; Aizebeokhai and Olayinka 2011; Nwajide, 2013). Current massive oil discoveries in the deep-water zones of the Niger Delta suggest that the province will continue to be a focus of exploration activities (Corredor et al. 2005). It has, therefore, become necessary to apply exploration and production technologies to harness these hydrocarbon resources. Many literatures have reported interesting petrophysical evaluation studies in the oil prolific area of the Niger Delta Basin, Nigeria (Omoboriowo, et al., 2012; Eshimokhai, and Akhirevbulu, 2012; Adizua, and Oruade, 2018; Osinowo, et al., 2017). Moreover, there is scarce literature on wells 025 and 029 of Fuba field. Eshimokhai, and Akhirevbulu, (2012) discovered the petroleum potential and attempt to make available the petrophysical results for the various reservoirs in three wells selected for enhanced characterization of the reservoir sands. Petrophysical evaluation reveal good porosity (0.26-0.34), water saturation (0.09-0.32) and hydrocarbon saturation (0.77-0.83). Adizua, and Oruade, (2018) identified two viable hydrocarbon bearing reservoirs marked R1 and R2. The average reservoir thickness for R1 and R2 was 45 ft and 55 ft respectively. Both have great prospects to produce gas and oil.

This study is taken from Fuba Field, Onshore, Niger Delta, Nigeria. The ultimate deliverable of this study was petrophysical evaluation of selected wells (wells 025 and 029) using 3D seismic and well logs of the area. The production data of the field were obtained from these two wells. The study was carried out to confirm the presence of hydrocarbon in these two wells. The major components of the study are: (a) Petrophysical evaluation. (b) Well Correlation performed in order to determine the continuity of the reservoir sand across the field. (c) Seismic Interpretation which involves well-to-seismic tie, fault mapping

Middle East Journal of Applied Science & Technology (MEJAST)
Volume 7, Issue 1, Pages 174-184, January-March 2024

and horizon mapping. This aids in giving more insight into petrophysical evaluation of selected wells using 3D seismic and well logs.

2.0. Location and Geology of the Study Area

The proposed study area Fuba Field is located in the onshore Niger Delta region. Figure 1 shows the map of the Niger Delta region showing the study area while Figure 2 shows the base map showing well locations in the study area. The Niger Delta lies between latitudes 4° N and 6° N and longitudes 3° E and 9° E (Whiteman, 1982). The Delta ranks as one of the major oil and gas provinces globally, with an estimated ultimate recovery of 40 billion barrels of oil and 40 trillion cubic feet of gas (Adegoke et al., 2017). The coastal sedimentary basin of Nigeria has been the scene of three depositional cycles (Short and Stauble, 1967). The first began with a marine incursion in the middle Cretaceous and was terminated by a mild folding phase in Santonian time. The second included the growth of a proto-Niger delta during the Late Cretaceous and ended in a major Paleocene marine transgression. The third cycle, from Eocene to Recent, marked the continuous growth of the main Niger delta. A new threefold lithostratigraphic subdivision is introduced for the Niger delta subsurface, comprising an upper sandy Benin Formation, an intervening unit of alternating sandstone and shale named the Agbada Formation, and a lower shaly Akata Formation. These three units extend across the whole delta and each ranges in age from early Tertiary to Recent. They are related to the present outcrops and environments of deposition. A separate member of the Benin Formation is recognized in the Port Harcourt area. It is Miocene-Recent in age with a minimum thickness of more than 6,000ft (1829m) and made up of continental sands and sandstones (>90%) with few shale intercalations (Horsfall et al., 2017). Subsurface structures are described as resulting from movement under the influence of gravity and their distribution is related to growth stages of the delta (Ochoma et al., 2020). Rollover anticlines in front of growth faults form the main objectives of oil exploration, the hydrocarbons being found in sandstone reservoirs of the Agbada Formation. The oil in geological structures in the basin may be trapped in dip closures or against a synthetic or antithetic fault.

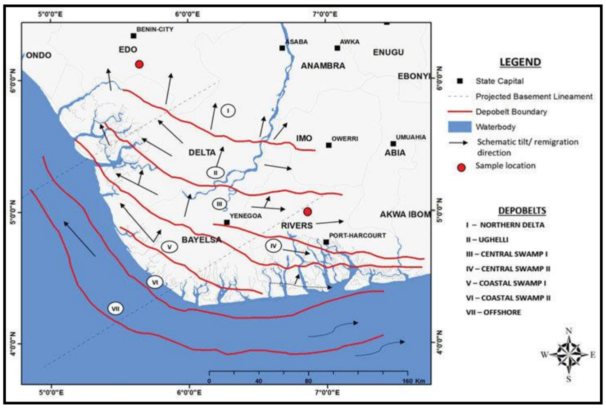

Figure 1. Map of Niger Delta Showing the study Area

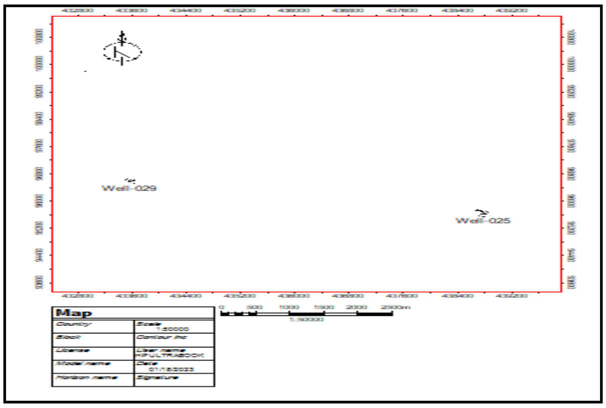

Figure 2. Base Map Showing Well Locations in the Study Area

3.0. Materials and Methods

This study makes use of wire line log as well as 3D seismic data. The well log data comprise of a suite of logs; gamma ray, neutron, density, deep resistivity and sonic logs for two wells. These were key in establishing the reservoir distribution and lateral continuity of the reservoirs in the study area. The interactive Petrel software was used for the study.

3.1. Well-Log and Seismic Data Quality Control

Well correlation involves lithologic description, picking top and base of sand-bodies, fluid discrimination and then linking these properties from one well to another based on similarity in trends. Correlation of reservoir sands was achieved using the

top and base of reservoir sands picked. The correlation process was possible based on similarity in the behaviour of the gamma ray log. In the Niger Delta, the predominant lithologies are sands and shales. In order to discriminate between these two lithologies in the subsurface, the gamma ray log is used. The gamma ray log reflects the shale content of sedimentary formations. Clean sandstones and carbonates normally exhibit a low level of natural radioactivity, while clay minerals and fluid particles in shales show higher levels of radioactivity due to adsorption of the heavy radioactive elements (Tiab, and Donaldson, 2004).

After defining the lithologies, the resistivity log was used for discriminating the type of fluid occurring within the pores in the rocks. The resistivity log can easily differentiate water from oil because water is conductive and oil is resistant to flow of electrical current. Hence, on the resistivity log, a sharp increase (a kick) in the resistivity measurement indicates the presence of hydrocarbons. The neutron and density cross-over (balloon effect) is often used to differentiate oil from gas in a reservoir. There was no gas present in any of the reservoir sands.

There are four basic steps involved in seismic interpretation relevant to this study and they include well-to-seismic ties, Fault Mapping, Horizon mapping and Petrophysical evaluation. The sonic log, which is the reciprocal of velocity, was calibrated using the checkshot data. The calibration process is necessary in order to improve the quality of the sonic log because the sonic log is prone to washouts and other wellbore related issues. The results of calibrating the sonic log with the checkshot gives the calibrated sonic log.

The calibrated sonic log is used along with the density log to generate an acoustic impedance (AI) log. The acoustic impedance log is calculated for each layer of rock. The next step involves generating the reflectivity coefficient (RC) log. The RC is calculated and generated using the AI log. The RC log generated is then convolved with a wavelet to generate a synthetic seismogram which is comparable with the seismic data. The statistical wavelet utilized for convolution is extracted from the seismic data. The synthetic seismogram was generated. The mathematical expressions that govern the entire well-to-seismic tie workflow are presented below:

$$AI = \rho v \qquad (1)$$

$$RC = \frac{\rho_2 v_2 - \rho_1 v_1}{\rho_2 v_2 + \rho_1 v_1} \qquad (2)$$

$$\text{Synthetic Seismogram} = \frac{\rho_2 v_2 - \rho_1 v_1}{\rho_2 v_2 + \rho_1 v_1} * wavelet \qquad (3)$$

where AI = acoustic impedance, RC = reflection coefficient, ρ = density; v = velocity.

Faults were identified as discontinuities or breaks in the seismic reflections. Faults were mapped on both inline and cross-line directions. Horizons are continuous lateral reflection events that are truncated by fault lines. The horizon interpretation process was conducted along both inline and crossline direction.

3.2. Petrophysical Evaluation

Petrophysics is the study of rock properties and their interactions with fluids (gases, liquid hydrocarbons, and aqueous solutions). In petroleum studies, petrophysical properties are those properties of the reservoir which enable the reservoir rocks to store and transmit reservoir fluids thus also enabling quantitative determination of the in-situ hydrocarbon as well as the appropriate formations method of extraction of the fluids. Four main petrophysical parameters are important in defining any reservoir, which include: shale volume (V_{SH}), total and effective porosity ($Ø_T$ and $Ø_E$), Net to Gross (NTG), permeability (K) and water saturation (S_W). Various equations applicable to the Niger Delta were utilized for their computation in this study.

3.2.1. Shale Volume (V_{SH})

This is the space occupied by shale or the fraction of shale (clay), present in reservoir rock (Cannon, 2018). The volume of shale is determined from mathematical correlations and gamma ray index. In mathematical equations, the volume of shale is represented as V_{SH}. The gamma ray index (GR_{index}) was first calculated in order to calculate the shale volume based on Schlumberger (1974) empirical equation as follows;

$$\mathrm{GR}_{\mathrm{index}} = \frac{GR_{log} - GR_{min}}{GR_{max} - GR_{min}} \qquad (4)$$

Where;

$GR_{log} = GR\ log\ reading\ of\ formation, GR_{min} = GR\ sand\ baseline$ and

$GR_{max} = GR\ shale\ baseline$

The Larionov (1969) equation for tertiary reservoirs was utilized for calculating the shale volume as follows;

$$\mathrm{Vsh} = 0.083 \times (2^{(3.7 \times GR_{index})} - 1) \qquad (5)$$

3.2.2. Effective Porosity

The effective porosity is the porosity that is responsible for flow to occur within the reservoir. Effective porosity (Φ_E) was calculated using volume of shale (Vsh) and total porosity (Φ_T) as follows (Dresser, 1979);

$$\emptyset_E = (1 - Vsh) \times \emptyset_T \qquad (6)$$

Where; $\emptyset_E = Effective\ porosity, \emptyset_T = Total\ Porosity, Vsh = Volume\ of\ shale$

3.2.3. Water Saturation

This is the relative extent to which the pores in rocks are filled with water. Saturation is expressed as the fraction, or percent, of the total pore volume occupied by the oil, gas, or water. Water saturation is denoted as Sw and is expresses in percent or fraction. Water saturation is predominantly controlled by porosity and formation resistivity. It can be calculated using Archies (1942) empirical model as follows;

$$Sw = \left(\frac{a \times R_w}{R_t \times \emptyset_t^m}\right)^{1/n} \qquad (7)$$

Where;

Sw = Archie's water saturation for clean sand

a = tortuosity factor = 1

m = cementation exponent = 2

n = saturation exponent = 2

Rt= formation resistivity (read from log)

Rw = formation water resistivity (read from log)

ϕt = total porosity

3.2.4. Hydrocarbon Saturation

The hydrocarbon saturation was calculated as follows;

$$S_H = (I - S_w) \qquad (8)$$

Where; S_H = hydrocarbon saturation and S_W = Archie's water saturation for clean sand

3.2.5. Permeability

$$K = \upsilon \frac{\mu \Delta x}{\Delta P} \qquad (9)$$

Where; K =permeability, υ = fluid velocity, μ =dynamic viscosity, Δx =thickness of the bed of the porous medium and ΔP = applied pressure difference.

3.2.6. Petrophysical Attribute Maps

Petrophysical attribute maps are seismic models which can be used to validate the static reservoir models. It is a 2D map view which serves as a model for doing quality check on the 3D petrophysical models. To generate the maps, the average petrophysical parameters are used as input. Petrophysical attributes maps were generated for the horizons of interest.

4.0. Results and discussion

4.1. Production Data

The production and reservoir pressure reports are presented in Figures 3 and 4. Production decline of 1192.21bbl/day resulted from pressure decline of 95.50bar/year or 0.062psi/year.

4.2. Reservoir Identification and Correlation

The results for lithology and reservoir identification are presented in (Figure 5). Two sand bodies (Q and R) were identified and correlated across two wells in the field. Both reservoir sands were used for the purpose of this study (Q and R). The resistivity logs which reveals the presence of hydrocarbons were used to identify the hydrocarbon bearing sands. On (Figure 5), the sands are coloured yellow while shales are grey in colour. Well-to-seismic tie was conducted on Fuba field using density log, sonic log and checkshot quality check for Well-1 is presented in Figure 6. A statistical wavelet (ISIS time) was used to give a near perfect match between the seismic and synthetic seismogram.

4.3. Fault and Horizon Interpretation

The results for the interpreted faults in Fuba field are presented in Figure 7 shows both synthetic and antithetic faults interpreted along seismic inlines. Faults are more visible along the inline direction because this direction reveals the true dip position of geologic structures. All interpreted faults are normal synthetic and antithetic faults. A total of thirty-six faults were interpreted across the entire seismic data. Of the interpreted faults, only F1 (synthetic fault) and F16 (antithetic fault) faults are regional, running from the top to bottom across the field. Hence, these faults play significant roles in trap formation at the upper, middle and lower sections of the field. The results for the interpreted seismic horizons (Horizons Q and R) are also presented in Figure 7.

4.4. Petrophysical Evaluation

The results of petrophysical evaluation conducted on reservoir sands Q and R are presented in Figure 8-16 and Tables 1 and 2 respectively. Well section showing reservoir petrophysical properties and their averages are presented in Figures 8 and 9.

Middle East Journal of Applied Science & Technology (MEJAST)
Volume 7, Issue 1, Pages 174-184, January-March 2024

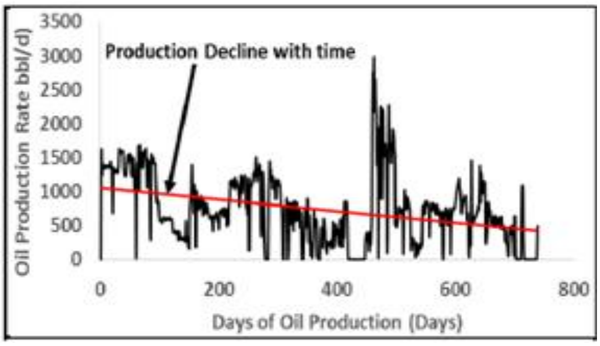

Figure 3. Reservoir Production Rate Versus Days of Oil Production

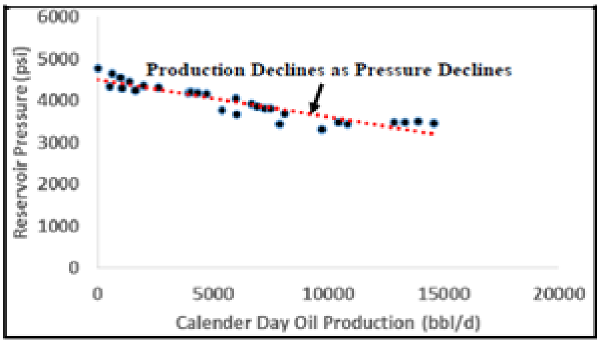

Figure 4. Effect of Reservoir Pressure Decline on Production

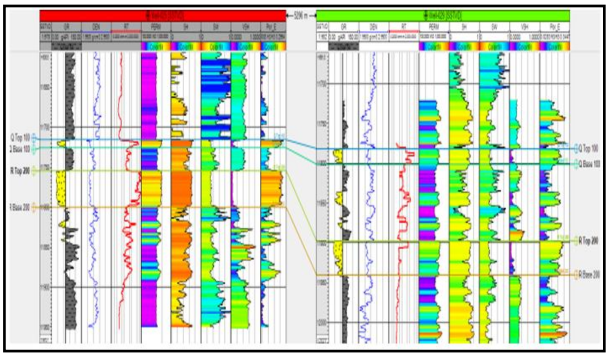

Figure 5. Well section showing reservoir identified and correlated across Fuba Field

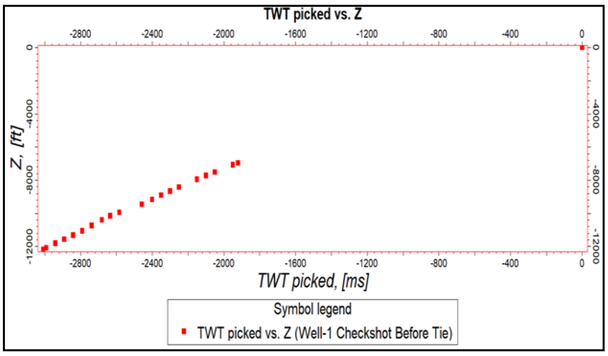

Figure 6. Checkshot Quality check for Well-1

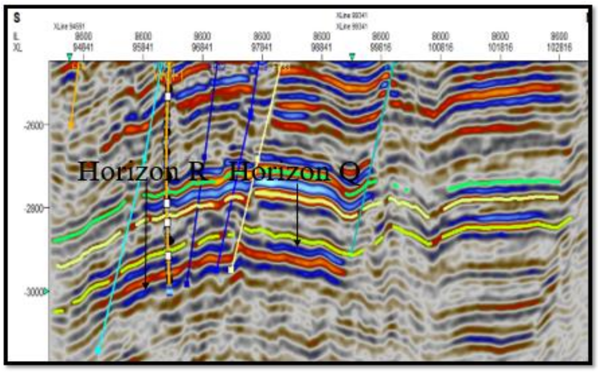

Figure 7. Faults and horizons interpreted along seismic inline section

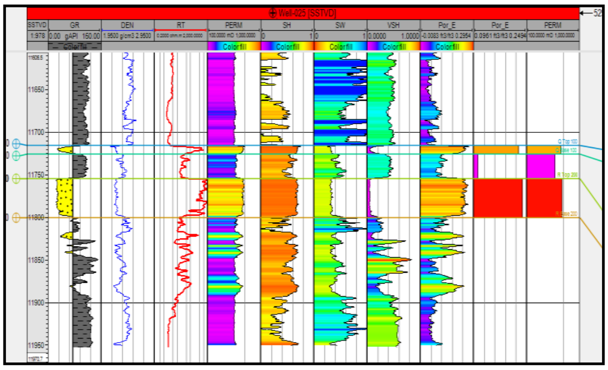

Figure 8. Well Section Showing Petrophysical Properties and their Averages for Well-025

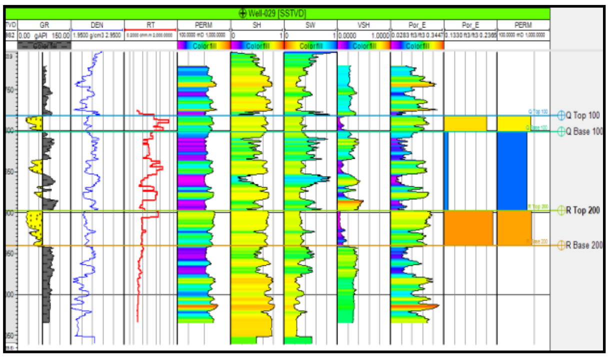

Figure 9. Well Section Showing Reservoir Petrophysical Properties and their Averages for Well-029

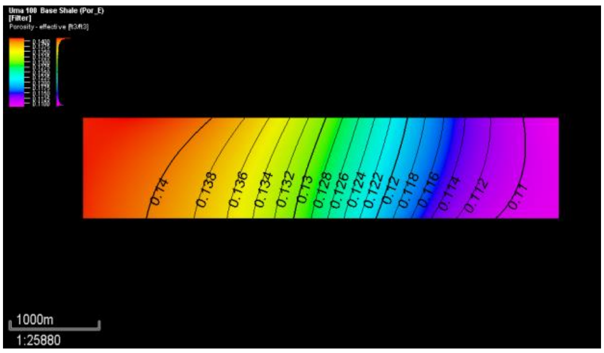

Figure 10. Shale Volume Map for Wells 025 and 029 (Reservoir Sand Q)

MEJAST
Middle East Journal of Applied Science & Technology (MEJAST)
Volume 7, Issue 1, Pages 174-184, January-March 2024

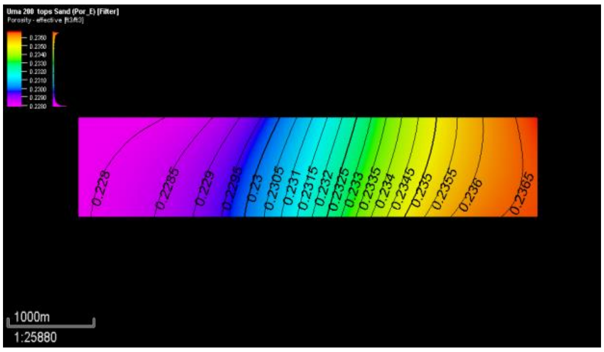

Figure 11. Porosity Map for Wells 025 and 029 (Reservoir Sand Q)

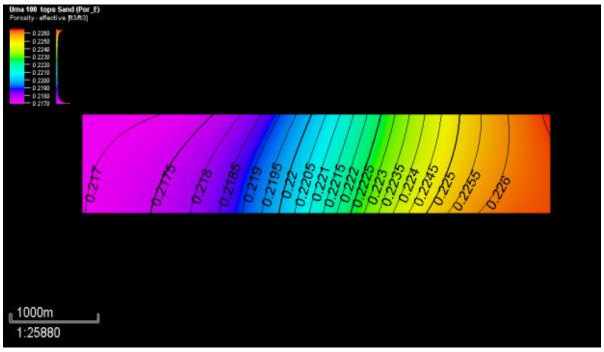

Figure 12. Porosity Map for Wells 025 and 029 (Reservoir Sand R)

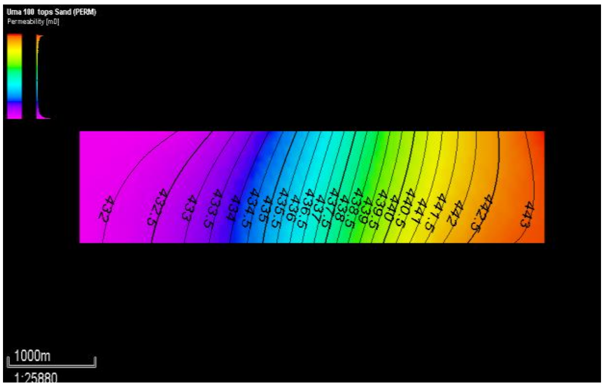

Figure 13. Permeability Map for Wells 025 and 029 (Reservoir Sand R)

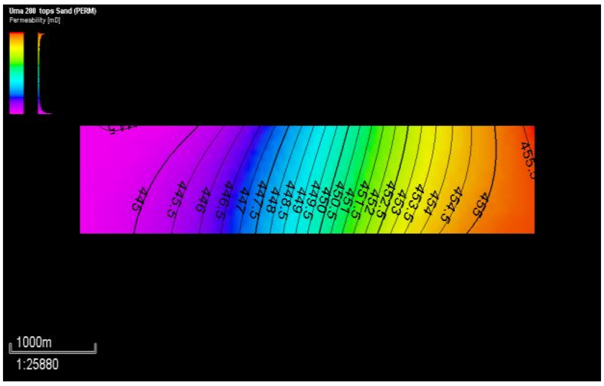

Figure 14. Permeability Map for Wells 025 (Reservoir Sand Q)

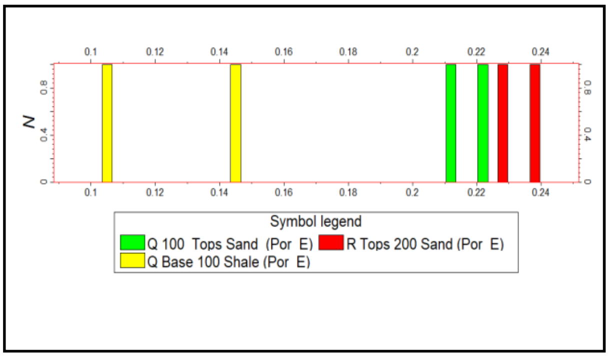

Figure 15. Histogram of Average Shale Volume and Average Effective Porosity for Wells 025 and 029

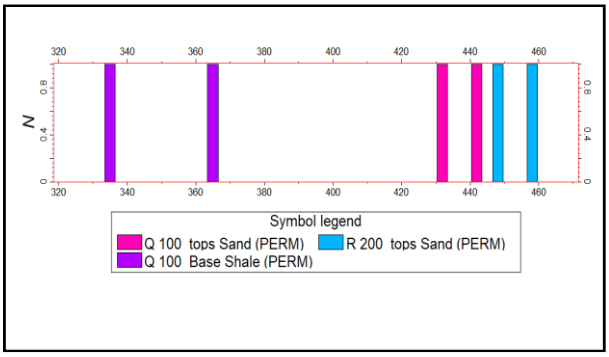

Figure 16. Histogram of Average Permeability for Wells 025 and 029

Table 1. Petrophysical Attributes Evaluation Data Table for Reservoir Q

Petrophysical Attributes						
Wells	**Net Thickness (H) (MD ft)**	**SH (%)**	**SW (%)**	**Effective Porosity (%)**	**Permeability (mD)**	**Shale Volume (%)**
Well_025	7.00	69.00	31.00	23.40	438.00	12.00
Well_029	20.00	70.00	30.00	23.60	440.00	13.00
Averages	13.50	69.50	30.50	23.50	439.00	12.50

Table 2. Petrophysical Attributes Evaluation Data Table for Reservoir R

	Petrophysical Attributes					
Wells	**Net Thickness (H) (MD ft)**	**SH (%)**	**SW (%)**	**Effective Porosity (%)**	**Permeability (mD)**	**Shale Volume (%)**
Well_025	48	68.00	32.00	22.00	452.00	15.00
Well_029	42	68.00	32.00	22.40	454.00	18.00
Averages	45	68.00	32.00	22.20	453.00	16.50

4.4.1. Net Thickness

The reservoir net thickness which is the clean sand portion of the reservoir ranges from 7.00 to 20.00 ft in reservoir sand Q (Table 1) and 42.00 to 48.00 ft in reservoir sand R (Table 2). In reservoir sand Q, well 029 showed higher net thickness than well 025 (Table 1). While, in reservoir sand R, well 025 showed higher net thickness than well 029 (Table 2). On average net sand thickness is 13.50 ft and 45.00 ft in reservoir sand Q and reservoir sand R respectively (Figure 2). These results show that sufficient thickness of the reservoirs are available as net sands (clean producible sand, provided they contain hydrocarbons).

4.4.2. Shale Volume

The shale volume ranges from 12.00 to 13.00% in reservoir sand Q (Table 1) and 15.00 to 18.00% in reservoir sand R (Table 2). In both reservoir sand Q and reservoir sand R, well 029 showed higher shale volume than well 025 (Tables 1 and 2). The average shale volume is 12.50% and 16.50% in reservoir sand Q and reservoir sand R respectively. These results show that the fraction of shale in the reservoirs is quite low.

4.4.3. Effective Porosity

Also, effective porosity ranged from 22.00 to 22.40% in reservoir sand Q (Table 1) and 23.40 to 23.60% in reservoir sand R (Table 2). In reservoir sand Q, well 025 showed higher effective porosity while the least effective porosity was found in well 029. In reservoir sand R, well 029 showed higher effective porosity, while lower effective porosity was found in well 025. On average, effective porosity values are 22.20 and 23.50% in reservoir sand Q and reservoir sand R (Tables 1 and 2). The porosity that is responsible for flow and accumulation in a reservoir is the effective porosity. Rocks have negligible porosity when < 5%, poor porosity when >5-10%, good porosity when >10-20%, very good when >20-30%, and excellent when >30 (Levorsen, 1967). Based on this classification scheme, the average effective porosity recorded for reservoir sand Q and R respectively is classed as very good. These results suggest that the reservoirs are porous enough to allow for accumulation of hydrocarbons.

4.4.4. Permeability

The results of reservoir permeability ranges from 438.00 to 440.00 mD in reservoir sand Q reservoir (Table 1) and 452.00 to 454.00 mD in Sand R reservoir (Table 2). In reservoir sand Q and reservoir sand R, well 029 showed higher permeability, while lower permeability was found in well 025. The average permeability values recorded in reservoir sand Q and reservoir sand R are 439.00 mD and 453.00 mD. On average, permeability in both reservoirs are greater than 250 mD but less than 1000

mD. Rider (1986) classified reservoir quality based on permeability values are as follows; < 10 mD (poor to fair), >10-50 mD (moderate), >50-250 mD (Good), >250-1000 mD (very good) and >1000 mD (excellent). Based on this classification scheme, reservoir sand Q and R are classed as having very good quality. These values are typical of Niger Delta reservoirs. Hence, fluid flow within these reservoir units will occur with ease because of the relatively high permeability values.

4.4.5. Fluid Saturation

Water saturation ranged from 30 to 31% in reservoir sand Q reservoir (Table 1) and 32% in reservoir sand R (Table 2). In reservoir sand Q, well 025 showed higher water saturation, while lower water saturation was found in well 029. In reservoir sand R, both well 025 and well 029 showed water an equal level of water saturation of 32%. On average, water saturation in the hydrocarbon reservoirs is 30.50 and 32% for reservoir sand Q and R respectively. This leads to a corresponding hydrocarbon saturation of 69.50 and 68% in reservoir sand Q and reservoir sand R. Based on these results, reservoir sand Q has higher hydrocarbon saturation than reservoir sand R. These hydrocarbon saturation values are good for reservoir development for production.

4.4.6. Petrophysical Attributes Maps and Histogram plots for Well 025 and 029

The shale volume map for wells 025 and 029 (Figure 10) indicates how the shale volume varies across the reservoirs. It ranges from 11% (purple) to 14% (yellow) on sand Q. This indicates that the fraction of shale in the reservoir is quite low. The porosity maps (Figures 11 and 12) indicate how the porosity varies across the reservoirs. It ranges from 21.7% (purple) to 22.6% (yellow) on sand Q and 22.8% (purple) to 23.65 (orange) in sand R. The permeability maps (Figures 13 and 14) indicate that permeability ranges from 432 (purple) to 443 mD (orange) on reservoir Q and 445 (purple) to 455 mD (orange) on reservoir R.

Figure 15 shows the histogram of average shale volume and average effective porosity for Wells 025 and 029 while Figure 16 shows the histogram of average permeability for wells 025 and 029.

5.0. Conclusion

Well-log data from two selected wells were used to evaluate petrophysical properties in Fuba Field in the onshore Niger Delta, Nigeria. The structural interpretation of seismic data reveal highly synthetic and antithetic faults which are in line with faults trends identified in the Niger Delta. Of the 36 interpreted faults, only synthetic and antithetic faults are regional, running from the top to bottom across the field. These faults play significant roles in trap formation at the upper, middle and lower sections of the field. A suite of well logs comprising gamma ray, deep resistivity, density, sonic and neutron were used in the analysis. Petrophysical properties evaluated are; thickness, porosity, permeability, water saturation and hydrocarbon saturation. Two reservoir sands were delineated and linked across two wells. The lithostratigraphy correlation section revealed that each of the sand units spread over the field differ in thickness with some units occurring at greater depth than their adjacent unit, that is possibly an evidence of faulting. Reservoir Q is found at a shallower depth from 11747.50 to 11761 ft, while reservoir R is found at a deeper depth ranging from 11825 to 11870 ft respectively. The two hydrocarbon reservoirs showed lateral continuity across the wells and fall within the Agbada formation where most of the hydrocarbon is believed to be trapped. From the result of Petrophysical evaluation, on average, net thickness, effective porosity, permeability, water saturation, hydrocarbon saturation and shale volume values are 13.50 ft, 23.50%, 463.70 mD, 30.50%, 69.50% and 12.50% for reservoir sand Q and 45.00 ft, 22.20%, 495.24 mD, 32% and 68% and 16.50% for reservoir sand R. The porosity and permeability values have been classed as good to excellent for reservoir sand Q and R respectively. The hydrocarbon saturation and water saturation values are good for reservoir development for production. The results of the sand-shale lithology calculated indicate the following (i) the fraction of shale in the reservoirs is quite low; (ii) sandstone volume decreased with increasing depth while shale volume increased with depth; (iii) an inverse relationship between permeability and shale volume and a direct relationship between

permeability and the volume of sand in the reservoirs. This is typical of clastic reservoir systems in the Niger Delta. An analysis of the petrophysical attributes maps indicates how the petrophysical qualities vary across the reservoirs. The results for this work can be used as an exploration tool for the identification of prospective areas and for feasibility studies during an appraisal activity in the study area.

Declarations

Source of Funding

This study did not receive any grant from funding agencies in the public, commercial, or not-for-profit sectors.

Competing Interests Statement

The author declares no competing financial, professional, or personal interests.

Consent for publication

The author declares that she consented to the publication of this study.

Acknowledgements

The author is grateful to Shell Petroleum Development Company of Nigeria (SPDC), Port Harcourt Nigeria for the release of the academic data for the purpose of this study.

References

[1] Etu-Efeotor, J.O. (1997). Fundamentals of Petroleum Geology. Paragraphics: Port Harcourt, PH.

[2] Adeoye, T.O., & Enikanselu, P.A. (2009). Hydrocarbon Reservoir Mapping and Volumetric Analysis using Seismic and Borehole Data over ‘‘Extreme’’ Field, South-western Niger Delta. Ozean Journal of Applied Sciences, 2(4): 429–441.

[3] Aizebeokhai, A.P., & Olayinka, I. (2011). Structural and Stratigraphic Mapping of EMI Field, Offshore Niger Delta. Journal of Geology and Mining Research, 3(2): 25–38.

[4] Nwajide, C.S. (2013). Geology of Nigeria’s Sedimentary Basins. CSS Bookshops Limited, Lagos.

[5] Corredor F., Shaw J.H., & Bilotti, F. (2005). Structural Styles in the Deepwater Fold and Thrust Belts of the Niger Delta. Association of Petroleum Geologists Bulletin, 89: 753–780.

[6] Omoboriowo, A.O., Chiaghanam, O.I., Chiadikobi, K.C., Oluwajana, O.A., Soronnadi-Ononiwu, C.G., & Ideozu, R.U. (2012). Reservoir Characterization of KONGA Field, Onshore Niger Delta, Southern Nigeria. International Journal of Science and Emerging Technology, 3(1): 19–30.

[7] Eshimokhai, S., & Akhirevbulu, O.E. (2012). Reservoir Characterization Using Seismic and Well Logs Data (A Case Study of Niger Delta). Ethopian Journal of Environmental Studies and Management, 5(4): 597–603.

[8] Adizua, O.F., & Oruade, L. (2018). Reservoir Characterization of an offshore Niger Delta “X” Field Using Well Log Data. International Journal of Engineering, Applied Science and Technology, 2(12): 1–4.

[9] Osinowo, O.O., Ayorinde, O.J., Nwankwo, P.C., Ekeng, O.M., & Taiwo, O.B. (2017). Reservoir Description and Characterization of Eni Field Offshore Niger Delta, Southern Nigeria. Journal of Petroleum Exploration Production Technology, 8(55): 1–17.

[10] Whiteman, A. (1982). Nigeria: Its Petroleum Ecology Resources and Potential. London, Graham and Trotman.

[11] Adegoke, O.S., Oyebamiji, A.S., Edet, J.J., Osterloff, P.L., & Ulu, O.K. (2017). Cenozoic Foraminifera and Calcareous Nannofossil Biostratigraphy of the Niger Delta. Elsevier, Cathleen Sether, United States.

[12] Short, K.C., & Stable, A.J. (1967). Outline of Geology of Niger Delta. Bulletin of America Association of Petroleum Geologists, 51(5): 761–779.

[13] Horsfall, O.I., Uko, E.D., Tamunoberetonari I., & Omubo-Pepple, V.B. (2017). Rock-Physics and Seismic-Inversion Based Reservoir Characterization of AKOS FIELD, Coastal Swamp Depobelt, Niger Delta, Nigeria. IOSR Journal of Applied Geology and Geophysics, 5(4): 59–67.

[14] Ochoma, U., Uko, E.D., & Horsfall, O.I. (2020). Deterministic Hydrocarbon Volume Estimation of the Onshore Fuba Field, Niger Delta, Nigeria. IOSR Journal of Applied Geology and Geophysics, 8(1): 34–40.

[15] Tiab, D., & Donaldson, E.C. (2004). Petrophysics: Theory and Practice of Measuring Reservoir Rock and Fluid Transport, 2nd edition. 2001 Gulf Professional Publishing, U.S.A.

[16] Cannon, S. (2018). Reservoir Modelling: A Practical Guide. John Wiley and Sons, Inc., 111 River Street, Hoboken, NJ 07030, USA.

[17] Schlumberger Well Services (1974). Log Interpretation Charts, Schlumberger Educational Services, New York, 83.

[18] Larionov, V. (1969). Borehole Radiometry: Moscow, U.S.S.R., Nedra.

[19] Dresser, A. (1979). Log Interpretation Charts, Dresser Industries Inc., Houston, Texas: 107.

[20] Archie, G.E. (1942). The Electrical Resistivity Log as an Aid in Determining some Reservoir Characteristics. Journal of Petroleum Technology, 5: 54–62.

[21] Levorsen, A.I. (1967). The geology of petroleum, 2nd edition. Freeman, San Francisco, Page 724.

[22] Rider, M.H. (1986). The Geological Interpretation of Well Logs. John Wiley and sons, Inc., New York.